

# Molecular dynamics simulation of SWCNT–polymer nanocomposite and its constituents

Ahmed Al-Ostaz · Ghanshyam Pal ·  
P. Raju Mantena · Alex Cheng

Received: 31 March 2007 / Accepted: 27 August 2007 / Published online: 29 September 2007  
© Springer Science+Business Media, LLC 2007

**Abstract** Elastic and engineering properties of nanoparticle enhanced composites and their constituents (matrix, reinforcement and interface) are calculated. The nanocomposites considered in this study consist of a single-wall carbon nanotube (SWCNT) embedded in polyethylene matrix. Molecular dynamics simulations are used to estimate the elastic properties of SWCNT, interfacial bonding, polyethylene matrix and composites with aligned and randomly distributed SWCNTs. The elastic properties of bundles with 7, 9, and 19 SWCNTs are also compared using a similar approach. In all simulations, the average density of SWCNT–polymer nanocomposite was maintained in the vicinity of CNTs, to match the experimentally observed density of a similar nanocomposite. Results are found to be in good agreement with experimentally obtained values by other researchers. The interface is an important constituent of CNT–polymer composites, which has been modeled in the present research with reasonable success.

## Nomenclature

$H$  Hamiltonian of the system  
 $\Psi$  Wave function  
 $R$  Position vector of atomic nucleus

$r_i$  Position vector of an electron in the atom (or any particle in general)  
 $\Theta$  Force field  
 $m$  Mass of the particle  
 $t$  Time  
 $E_{\text{total}}, U$  Total potential energy of the system  
 $K_2, K_3, K_4$  Force constants associated with bond length change  
 $b$  Changed bond length  
 $b_o$  Equilibrium bond length  
 $K_{2\theta}, K_{3\theta}, K_{4\theta}$  Force constants associated with bond angle change  
 $\theta$  Changed angle between two bonds  
 $\theta_o$  Equilibrium angle between two bonds  
 $K_{1\phi}, K_{2\phi}, K_{3\phi}$  Force constants associated with bond torsion  
 $\phi$  Torsion angle  
 $K_{2\chi}$  Force constants associated with out of plane angle change  
 $\chi$  Out of plane angle  
 $\chi_o$  Equilibrium out-of-plane angle  
 $K_{b\theta}$  Force constants associated with bond length change and bond angle change coupling  
 $K_{1b}, K_{2b}, K_{3b}$  Force constants associated with bond length change and bond torsion coupling  
 $K_{1\theta\phi}, K_{2\theta\phi}, K_{3\theta\phi}$  Force constants associated with bond angle change and bond torsion coupling  
 $K_{\theta\phi}$  Force constants associated with second order bond angle change and bond torsion coupling  
 $e$  Charge of an electron  
 $C_{ijkl}$  Stiffness matrix  
 $\sigma_{ij}$  Stress component

A. Al-Ostaz (✉)  
Department of Civil Engineering, The University of Mississippi,  
202 Carrier Hall, University, MS 38677, USA  
e-mail: Alostaz@olemiss.edu

G. Pal · P. R. Mantena · A. Cheng  
Composite Structures and Nano Engineering Research Group,  
The University of Mississippi, University, MS 38677, USA

$\varepsilon_{kl}$	Strain component
$A$	Helmholtz free energy
$V$	Volume of the simulation cell
$V_0$	Undeformed volume of the simulation cell
$v$	Velocity of the particle
$f_i$	Force acting on the particle $i$
$p_i$	Momentum of the atom (particle) in original system
$\bar{F}, \bar{G}$	Trajectory average of any thermodynamic property
$N$	Total number of atoms in the system
$\rho_i$	Position vector in the scaled coordinate system
$Q$	Same as volume, $V$
$\eta, M$	Constants
$\pi_i$	Momentum conjugate to $\rho_i$
$\Pi$	Momentum conjugate to $Q$
$S$	Stochastic collision term for atoms
$\gamma$	Mean rate of stochastic collision
$C_{ij}$	Material stiffness matrix
$E_{ij}, \nu_{ij}, \mu_{ij}, K_{ij}$	Engineering constants (Young's modulus, Poisson's ratio, shear modulus and bulk modulus)
$E_{\text{pull-out}}$	Pull-out energy
$\tau_i$	Interfacial shear stress
$a$	Radius of the nanotube
$L$	Length of the nanotube

## Introduction

The emergence of nano-sciences during the last decade has drastically altered the landscape of scientific research and technology development. Nano reinforcement of engineering materials can impart dramatic structural (e.g., stiffness) and physical (e.g., reduced CTE) property benefits without adding significant weight [1, 2]. For example, nanolayered reinforcement can impart greater thermal stability [3, 4] with reduced permeability, making the polymer less flammable, and improving barrier performance [5–7]. Ideally, the nanolayer reinforcement distributes internal stresses more uniformly allowing greater dimensional latitude in forming and shaping processes compared to conventional macroscale reinforcement. The unparalleled characteristics of clay nanolayers to boost mechanical properties of an engineering polymer (Nylon-6) were first demonstrated by Toyota researchers [8]. With only 4.2 wt.% of clay nanolayers, the modulus doubled and heat distortion temperature increased by 80 °C compared to the pristine polymer, along with a reduction in water permeability and an increase in flame retardant properties. These dramatic improvements in properties made it possible to extend the use of low-cost

polymers in under-the-hood applications. In order to fully utilize this type of mechanical property improvement for structural applications, the resulting nanoreinforced composite materials must have high modulus, high heat deflection temperature, low thermal expansion coefficient, high tensile strength and low permeation rates.

A critical issue for nanotechnology is the ability to understand, model, and simulate the behavior of small structures and to make the connection between structure properties and functions. Most nanosystems are too small for direct measurements but too large to be described by current rigorous first principles in theoretical and computational methods. They exhibit too many statistical ensembles. This problem is even more challenging in the case of nanocomposites where carbon nanotubes are dispersed randomly in a polymeric (i.e., polystyrene, epoxy etc.) matrix. The vital role of molecular modeling in this field is to enable engineering design at the component and systems level, and to set objectives that could guide laboratory efforts of the physical implications. An important component in molecular mechanics calculations of nanostructured materials is the description of the forces between individual atoms which are characterized by force fields.

## Simulation of carbon nanotube composites using molecular dynamics approach

Many researchers have attempted to model the mechanical behavior of single wall carbon nanotube (SWCNT) taking input from molecular mechanics. Several new computational methods and their applications to nanostructures have been developed: equivalent continuum models [9–11], quasi-continuum models [12–18] using Tersoff and Brenner interatomic potential [19, 20], and molecular dynamics simulations [21, 22]. In this article we focus on modeling and simulation of SWCNT composites using the molecular dynamics approach.

### The Born–Oppenheimer approximation

The Born–Oppenheimer approximation is the foundation of molecular dynamics [23]. Noting that the electrons are several thousands of times lighter than the nuclei and therefore move much faster, Born and Oppenheimer proposed that the motion of the electrons can be decoupled from that of the nuclei, giving two separate equations. The first of these equations describes the electron motion where the energy is the function of coordinate of nucleus  $E(R)$  only and is termed as potential energy surface. The second part of the equation describes the motion of the nucleus on this potential energy surface. The solution of the nucleus

motion is the basis of molecular dynamics. But prior to that, one needs to solve the equation pertaining to the motion of the electron for the expression of the  $E(R; r)$ . Solving the equation for electronic motion is not easy because the potential energy surface is not unique. Thus, an empirical fit to the potential energy surface, commonly called a force field ( $E_{\text{total}}$ ), is usually used. Since the nuclei are relatively heavy objects, quantum mechanical effects are often insignificant and equation of motion for nuclei can be replaced by Newton's equation of motion given as:

$$-\frac{d\Theta}{dR} = m \frac{d^2R}{dt^2} \quad (1)$$

where,  $\Theta$  is the force field,  $R$  describes the location of the nuclei in space,  $m$  is the mass of the nuclei and  $t$  is time. The solution of the above equation is the term  $R(t)$  called the trajectory of the system.

### The force field

A force field in molecular mechanics and molecular dynamics is the average description of the existing interactions among various atoms in a molecule or a group of molecules in terms of functions and parameters sets [24]. The electronic configuration around atoms is not included into the description of these atomic interactions. Generally, the force field parameters are empirical, derived from quantum modeling and, sometimes, from heuristics.

The functional forms of various interactions, summed together in order to yield the COMPASS force field can be achieved from the introductory paper on COMPASS by Sun [25].

$$\begin{aligned} E_{\text{Total}} = & \sum_b [K_2(b - b_o)^2 + K_3(b - b_o)^3 + K_4(b - b_o)^4] \\ & + \sum_{\theta} [K_{2\theta}(\theta - \theta_o)^2 + K_{3\theta}(\theta - \theta_o)^3 + K_{4\theta}(\theta - \theta_o)^4] \\ & + \sum_{\phi} [K_{1\phi}(1 - \cos \phi) + K_{2\phi}(1 - \cos 2\phi) \\ & + K_{3\phi}(1 - \cos 3\phi)] + \sum_{\chi} K_{2\chi}(\chi - \chi_o)^2 \\ & + \sum_{b,\theta} K_{b\theta}(b - b_o)(\theta - \theta_o) + \sum_{b,\phi} (b - b_o)[K_{1b} \cos \phi \\ & + K_{2b} \cos 2\phi + K_{3b} \cos 3\phi] + \sum_{\theta,\phi} (\theta - \theta_o)[K_{1\theta\phi} \cos \phi \\ & + K_{2\theta\phi} \cos 2\phi + K_{3\theta\phi} \cos 3\phi] + \sum_{b,\theta} (\theta' - \theta'_o)(\theta - \theta_o) \\ & + \sum_{\theta,\theta,\phi} K_{\theta\phi}(\theta' - \theta'_o)(\theta - \theta_o) \cos \phi \\ & + \sum_{ij} \frac{q_i q_j e}{r_{ij}} + \sum_{ij} \epsilon_{ij} \left[ 2 \left( \frac{r_{ij}^o}{r_{ij}} \right)^9 - 3 \left( \frac{r_{ij}^o}{r_{ij}} \right)^6 \right] \quad (2) \end{aligned}$$

where the first 10 terms are “valence terms”. The first through fourth terms represent the energy associated with bond ( $b$ ), angle ( $\theta$ ), torsion ( $\phi$ ), and Wilson out-of-plane ( $\chi$ ) internal coordinates respectively. The rest of the terms excluding the last two terms represent the energies of cross-coupled internal coordinates which are important for calculating the vibration frequencies and structural variations associated with conformational changes. The last two terms represent “nonbond” interaction between atoms separated by two or more intervening atoms, or belonging to different molecules. The second-to-last term is the Coloumb potential that represents electrostatic interactions. The last term of Eq. 2, that is the Lenard-Johns 9-6 (LJ 9-6) potential, represents the van der Waals interaction. The LJ-9-6 function is considered as a soft function in the repulsive region compare to the conventional LJ-12-6 function.

### Simulation of SWCNT composites and their constituents

In this article we use commercially available molecular dynamics software (Materials Studio<sup>®</sup> 4.1) by Accelrys [23] to simulate a nanocomposite and its constituents (e.g., reinforcement, matrix, and interface). The nanocomposite considered in this study consists of a single-wall carbon nanotube (SWCNT) embedded in polyethylene matrix. Molecular dynamics approaches are used to estimate the elastic properties of SWCNT, interfacial bonding, polyethylene matrix, and composites with aligned and randomly distributed SWCNTs. The elastic properties of bundles of 7, 9, and 19 SWCNTs are also compared using the same approach.

For each configuration submitted for static elastic constants analysis, the first step consists of energy minimization using conjugate gradients method. In this study, the target minimum derivative for the initial step is 0.1 kcal/Å. However, to reduce the time required for the calculation, a maximum of 1,000 steps are performed in attempting to satisfy the convergence criterion. Following the initial stage, three tensile and three pure shear deformations of magnitude  $\pm 0.0005$  are applied to the minimized system and the system is re-minimized following each deformation. The internal stress tensor is then obtained from the analytically calculated virial, which is also used for obtaining estimates of the stiffness matrix.

As a result of these simulations, the elastic stiffness coefficients can be obtained by calculating  $\Delta\sigma_i/\Delta\epsilon_j$  for each of the applied strains, where  $\sigma_i$  represents, in vector notation, elements of the stress tensor obtained analytically using the following expression:

$$\sigma = -\frac{1}{V_o} \left[ \left( \sum_{i=1}^N m_i (v_i v_i^T) \right) + \left( \sum_{i<j} r_{ij} f_{ij}^T \right) \right] \quad (3)$$

where, index  $i$  runs over all particles 1 through  $N$ ;  $m_i$ ,  $v_i$  and  $f_i$  denote the mass, velocity and force acting on particle  $i$ ; and  $V_o$  denotes the (undeformed) system volume.

Due to scaling problems and computational limitations, one can simulate the behavior of only a small number of particles (few thousand atoms) by using molecular dynamics. However, in order to eliminate the surface effects and to simulate the bulk material, periodic boundary conditions are imposed on the system.

### Results and discussion

Molecular dynamics simulation of SWCNT–polymer constituents

#### Molecular dynamics simulation of SWCNT

One of the primary aims of the present study is to determine the elastic and/or engineering constants of single-wall carbon nano tubes of different chirality. Molecular dynamics simulation runs of SWCNT with (7,0) chirality (Fig. 1a) and (5,5) chirality (Fig. 1b) were carried out under the constant Number of particle, constant Pressure and constant Temperature (NPT) ensemble. These two chiralities were chosen because they have a similar radius of the CNT. The length of SWCNT was chosen as 105 Å so that an aspect ratio of 25:1 (length:diameter) could be maintained in order to capture the slender structure of SWCNTs. One SWCNT was then placed into a 105 Å × 8.7 Å × 8.7 Å simulation cell. The simulation parameters for NPT molecular dynamics of one SWCNT are given in Table 1.

Depending upon load conditions, the simulation was divided into three parts: axial, transverse, and shear loadings. The simulation cell was subjected to uniaxial tensile loading along the tube axis. The load was varied from  $2.0265 \times 10^{-2}$  MPa to  $1.01325 \times 10^2$  MPa during different simulation runs. In other simulation runs, the load was

applied either in the transverse or shear direction with load varied between  $2.0265 \times 10^{-2}$  MPa and  $1.01325 \times 10^2$  MPa during different simulation runs. All of the runs gave similar results. For each configuration submitted for static elastic constants analysis, a total of 13 minimizations are performed. The first consists of a conjugate gradients minimization of the undeformed amorphous system. The target minimum derivative for this initial step is 0.1 kcal/Å. However, to reduce the time required by the calculation, a maximum of 1,000 steps are performed in attempting to satisfy the convergence criterion. Following this initial stage, three tensile and three pure shear deformations of magnitude  $\pm 0.0005$  are applied to the minimized undeformed system and the system is re-minimized following each deformation. The internal stress tensor is then obtained from the analytically calculated virial and used to obtain estimates of the six columns of the elastic stiffness coefficients matrix. These are the default values in the software which are calculated automatically and this is why the choice of applied loading magnitude (as long as it is in the elastic limit) and direction are irrelevant. Typical elastic constants obtained for the case of 7,0 SWCNT are:

$$C_{ij} = \begin{bmatrix} 1027 & 25.18 & 19.45 & 0 & 0 & 0 \\ 26.78 & 43.11 & 20.54 & 0 & 0 & 0 \\ 20.33 & 28.08 & 37.43 & 0 & 0 & 0 \\ 0 & 0 & 0 & 7.28 & 0 & 0 \\ 0 & 0 & 0 & 0 & 5.59 & 0 \\ 0 & 0 & 0 & 0 & 0 & 7.14 \end{bmatrix} \text{ GPa}$$

and for the 5,5 SWCNT case are:

$$C_{ij} = \begin{bmatrix} 729.8 & 1.123 & 1.489 & 0 & 0 & 0 \\ 1.494 & 2.320 & .016 & 0 & 0 & 0 \\ 1.463 & 0.341 & 0.766 & 0 & 0 & 0 \\ 0 & 0 & 0 & 11.81 & 0 & 0 \\ 0 & 0 & 0 & 0 & 1.435 & 0 \\ 0 & 0 & 0 & 0 & 0 & 11.86 \end{bmatrix} \text{ GPa}$$

where  $i, j = 1, 2, 3$  with 1 representing the axial direction and 2, 3 representing plane of symmetry. Thus we have a

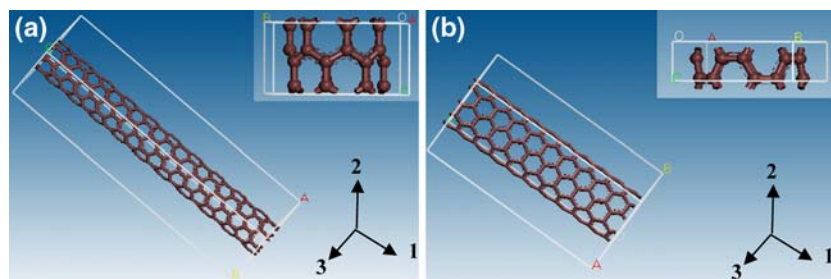


Fig. 1 Molecular dynamic simulation of SWCNT with (a) 7,0 chirality, and (b) 5,5 chirality

**Table 1** Molecular dynamics simulation parameters for one SWCNT

System	One (7,0) or (5,5) SWCNT, 105 Å length
MD ensemble	NPT
Temperature	293 K
Time step	1 femto second (fs)
Duration of simulation	100 pico second (ps)
Periodic boundary condition	ON

transversely isotropic problem. For this case, the five engineering constants may be calculated from elastic constants using the following relations [26]:

$$E_{11} = C_{11} - \frac{2C_{12}^2}{C_{22} + C_{23}}$$

$$E_{33} = E_{22} = C_{22} + \frac{C_{12}^2(-C_{22} + C_{23}) + C_{23}(-C_{11}C_{23} + C_{12}^2)}{C_{11}C_{22} - C_{12}^2}$$

$$\nu_{12} = \nu_{13} = \frac{C_{12}}{C_{22} + C_{23}}$$

$$\mu_{23} = \frac{1}{2}(C_{22} - C_{23})$$

$$K_{23} = \frac{1}{2}(C_{22} + C_{23})$$

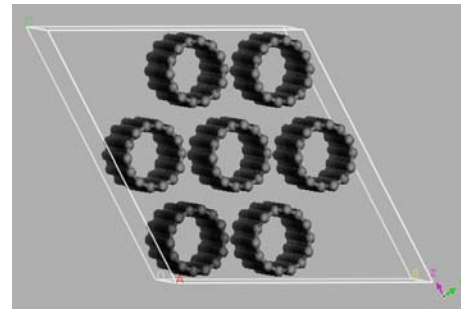
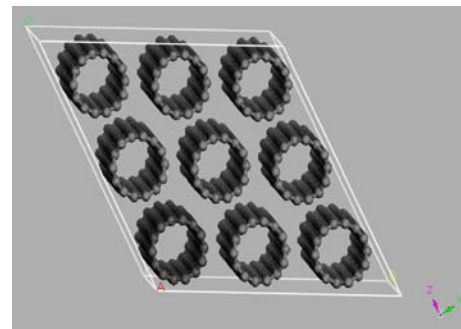
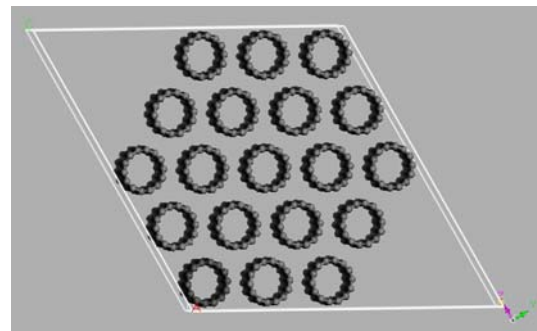
(4)

Thus, the axial Young's modulus of arm-chair CNT is 1007 GPa ( $\approx 1$  TPa) whereas the axial Young's modulus of zigzag CNT is 728 GPa. These are in good agreement with experimentally obtained values by other researchers [27].

#### Molecular dynamics simulation of clusters of SWCNT

Carbon nanotubes naturally tend to form crystals of hexagonally packed bundles or ropes that exhibit transversely isotropic behavior. Determination of the effective mechanical properties of nanotube bundles is important so that their applicability as reinforcements in composite materials can be evaluated. Also, once the effective properties of the carbon nanotube bundles are determined, these values can be used as input parameters for the next step in case of multi level modeling of SWCNT–polymer matrix composites. In these bundles, the inter-tube force interactions are due to primarily nonbonding Van der Waals interactions. These weak cohesive properties of nanotube bundles are important in the prediction of mechanical properties of nanotube composite materials and those of fibers of woven carbon nanotubes.

Three clusters of (7,0) SWCNTs were examined using molecular dynamics. The first cluster consists of seven

**Fig. 2** Cluster of seven (7,0) SWCNTs inside the simulation cell**Fig. 3** Cluster of nine (7,0) SWCNTs inside the simulation cell**Fig. 4** Cluster of 19 (7,0) SWCNTs inside the simulation cell

SWCNTs packed in hexagonal fashion in a simulation cell, the second cluster consists of nine, and third cluster consists of 19 SWCNTs packed in hexagonal fashion in a simulation cell as shown in Figs. 2, 3, and 4, respectively. Constant temperature–constant pressure (NPT) molecular dynamics was performed. In order to simulate normal temperature and pressure conditions during the simulation experiment, the temperature of the system was maintained at 298 K and an arbitrary chosen small hydrostatic pressure of magnitude 10 atm was applied on the simulation cell in all three experiments. The NPT MD simulation parameters are given in Table 2 and the results of MD simulation are reported in Table 3.

**Table 2** Molecular dynamics simulation parameters for SWCNT bundles

System	Cluster of (7,0) SWCNTs, 105 Å length
MD ensemble	NPT
Temperature	298 K
Time step	1 femto second (fs)
Duration of simulation	100 pico second (ps)
Periodic boundary condition	ON

*Molecular dynamics simulation of matrix*

Polyethylene, a thermoplastic, has been chosen as the matrix material for construction of the composite. Polyethylene [IUPAC name—polyethene (PE)] is a thermoplastic commodity polymer [28] created through polymerization of ethylene. Its name originates from the monomer ethene, also known as ethylene, used to create the polymer. The ethylene molecule, C<sub>2</sub>H<sub>4</sub> is CH<sub>2</sub>=CH<sub>2</sub>, two CH<sub>2</sub> connected by a double bond. The polymerized structure of the polyethylene is shown in Fig. 5.

Polyethylene is classified into several different categories based on its density and branching. Sometimes some of the carbons, instead of having hydrogen attached to them, they have long chains of polyethylene attached to them. This is called branched, or low-density polyethylene, or LDPE. When there is no branching, it is called linear polyethylene, or HDPE. Linear polyethylene is much stronger than branched polyethylene. The mechanical properties of PE depend significantly on variables such as the extent and type of branching, the crystal structure, and the molecular weight [28].

Simulation of the polymer consists of potential energy minimization followed by two steps of molecular dynamics. A single simulation cell of the polymer consists of eight chains of monomer comprising of total 1,216 atoms. This simulation cell was then subjected to periodic boundary conditions in order to simulate the behavior of the bulk polymer. Initially, during the actual chemical reaction the rate of the reaction is reported to be fast which gradually slows down as the chemical reaction proceeds. Therefore, in order to capture the complete trajectory of the polymer chains during molecular dynamics simulations, a two step molecular dynamics simulation was carried out.

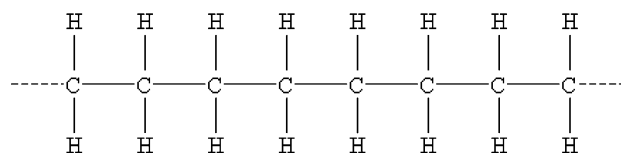


**Fig. 5** Polymerized structure of the polyethylene

The first stage of dynamics was carried out for 20 pico second (ps) with a smaller time step of 0.2 femto second (fs). This was followed by the second stage with a comparatively larger time step of 1.0 fs which lasted for 100 ps. The final density of the polymer matrix was maintained as 0.92 g/cc. The temperature of the system was maintained at 298 K throughout the simulation and a hydrostatic pressure of 1 atm pressure was applied to the system during the dynamics. Figures 6 and 7 show the polymer chains used in this simulation, and Table 4 shows final engineering properties of the simulated polymer system.

*Molecular dynamics simulation of the SWCNT–polymer interfacial bonding*

In case of composites, the effective transfer of load from matrix to reinforcement occurs via the interface. The extent of this load transfer depends upon the degree of adhesion between the nanotube and matrix material. The adhesive strength between the nanotubes and the polymeric matrix can be evaluated by the interfacial bonding energy. In case of nonfunctionalized SWCNT–polymer composites, the nature of interfacial bonding energy comes from electrostatic and Van der Waals force in the composite system.

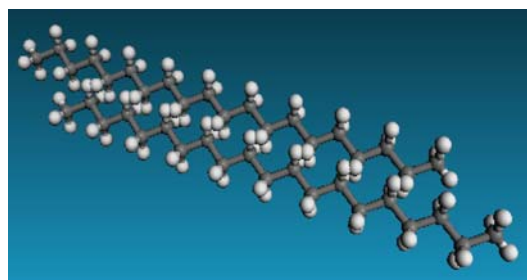


**Fig. 6** Simulated single polymer chain of polyethylene

**Table 3** Results of MD simulation of (7,0) SWCNT clusters

Simulation conditions	$E_{11}$ (GPa)	$E_{22}$ (GPa)	$\nu_{12}$	$\mu_{23}$ (GPa)	$K_{23}$ (GPa)
Seven nanotubes, NPT, 1.0 Mpa (hydrostatic), 293 K	1021.7	26.85	0.31	8.41	33.7
Nine nano-tubes (displaced from their equilibrium positions), NPT, 1.0 MPa (hydrostatic), 293 K	1019.6	19.49	0.29	5.73	32.88
19 nanotubes, NPT, 1.0 Mpa (hydrostatic), 293 K	931.3	14.96	0.29	4.44	23.9

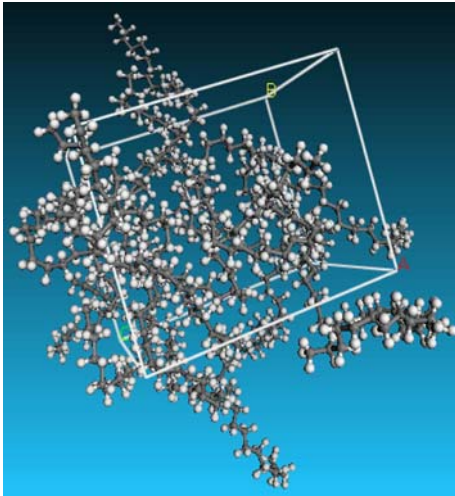


**Fig. 7** Simulated polymer chains of polyethylene

**Table 4** Engineering constants of the simulated polyethylene

$E$ (GPa)	$\nu_{12}$
1.22	0.37

**Fig. 8** Atomistic model of the composite for interfacial binding energy analysis

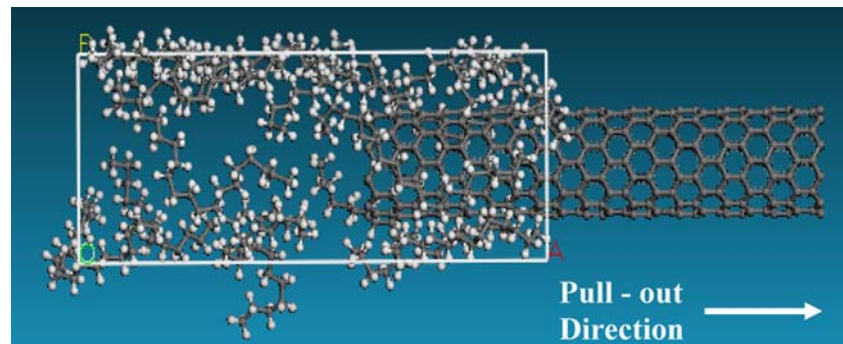
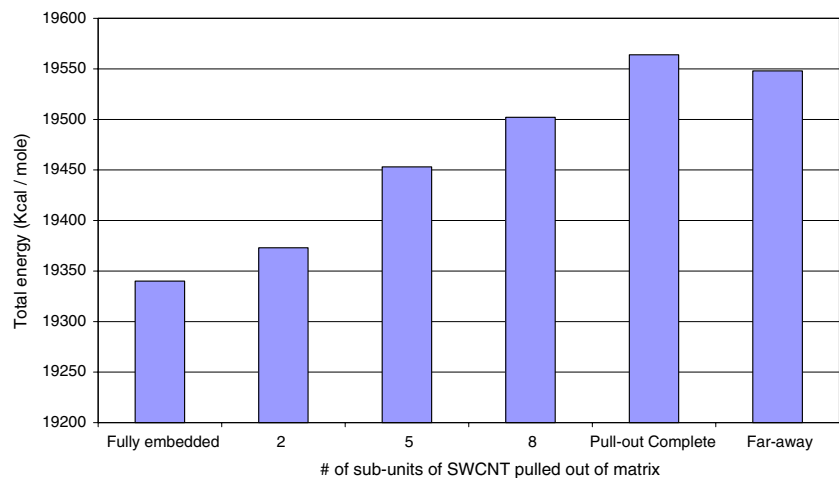


**Fig. 9** Potential energy variation for SWCNT pull-out test from polyethylene matrix in single SWCNT composite



Molecular dynamics simulation of the interface for SWCNT–polymer composite was carried out by simulating the single fiber pull-out test. Figure 8 shows the atomistic model used for interfacial binding simulations. The polymer composite model used in this study was 10,0 SWCNT–polyethylene composite. The model has a total of 1,206 atoms and the final density of the composite was 1.3 g/cc. Before the start of pull-out test, the periodic boundary conditions imposed on the system were removed. The total energy of the system increases as the SWCNT is pulled out of the composite. This increase in total energy can be attributed to an increase in the potential energy of the system due to the formation of new surfaces. Figure 9 shows the variation in total energy, essentially the potential energy, of SWCNT–polyethylene resin composite as a function of the number of sub-units of SWCNT pulled out of the composite. Once, the whole SWCNT is pulled out of the matrix, the variation in total energy attains a plateau as the SWCNT is left far away from the matrix, because in such a situation the interaction between matrix and SWCNT is extremely weak.

According to Gou et al. [29], the pull-out energy,  $E_{\text{pull-out}}$ , is defined as the energy difference between the fully embedded nanotube and the complete pull-out

configuration. It can be related to the interfacial shear stress,  $\tau_i$ , by the following relation:

$$E_{\text{pull-out}} = \int_0^L 2\pi a(l-x)\tau_i dx = \pi a\tau_i L^2 \tag{5}$$

$$\Rightarrow \tau_i = E_{\text{pull-out}}/\pi aL^2 \tag{6}$$

where,  $a$  and  $L$  are the radius and length of the nanotube, respectively, and  $x$  is the displacement of the nanotube.

The  $E_{\text{pull-out}}$  for the system comes out to be 224 kcal/mol. The radius of the (10, 0) nanotube is 7.875 Å and the length of the SWCNT in the present system was 42.26 Å. The interfacial shear strength for the system under consideration comes out to be 133 MPa. This value of interfacial strength is comparable to interfacial strength value of 150 MPa for nanotube–polystyrene system reported in literature [30].

In another set of simulations, the same system was subjected to periodic boundary conditions. But, because of periodic boundary conditions of the system, when a SWCNT is pulled out from one end, another SWCNT enters from the opposite end into the simulation cell from its neighboring image cell. Therefore, the total energy of the system remains almost unaffected. Therefore, effect of the SWCNT pulling on the total energy of the system could not be studied in such a scenario.

### Molecular dynamics simulation of SWCNT–polyethylene composite

A key problem in the case of CNT polymer composites is the bonding between CNT and polymer matrix. On the one hand, the Van der Waals forces are too weak to provide strong connections between CNT and the matrix such that attacks on CNT by chemical agents may result in development of covalent bonds with carbon atoms, which affect the structure of CNT. On the other hand, due to spatial mismatch between the atomic structure of CNT and matrix material, there can exist (by analogy with epitaxial growth)

significant residual stresses, which in turn may cause defects in the matrix and deformation of CNT. These factors can change key properties of the CNT such as electrical and thermal conductivity. Figure 10 illustrates the deformed shape of a CNT (departure from circularity of cross-section) when surrounded by polymer chains, as obtained from molecular dynamics simulation.

Molecular dynamics simulation was carried out for the SWCNT–polyethylene matrix composite. The simulation cell for the composite consists of single 7,0 SWCNT embedded in polyethylene matrix. The dimensions of the simulation cell were maintained as 100 Å × 50 Å × 50 Å. The two-step NPT molecular dynamics, described in Section “MD simulation of matrix material”, was applied to the present case as well. The temperature of the system was maintained at 298 K throughout the simulation and a hydrostatic pressure of 1 atm pressure was applied to the system. Figure 11 also shows the polymer chains used in this simulation and Table 5 shows final engineering constants of the simulated polymer system.

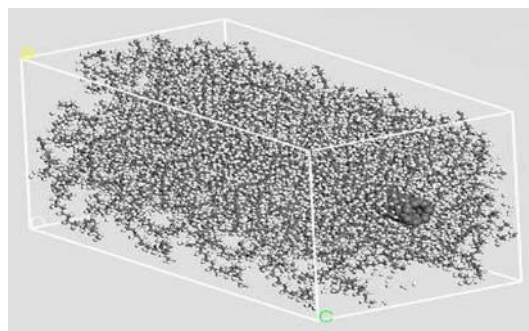


**Fig. 11** Molecular dynamics simulation cell for SWCNT–polyethylene matrix composite

**Table 5** Mechanical properties for SWCNT–polyethylene composite from molecular dynamics simulation

$E_{11}$ (GPa)	$E_{22}$ (GPa)	$\nu_{12}$	$\mu_{23}$ (GPa)	$K_{23}$ (GPa)
92.18	2.31	0.33	0.97	13.55

**Fig. 10** An arm chair CNT surrounded by ethylene molecules, before energy minimization

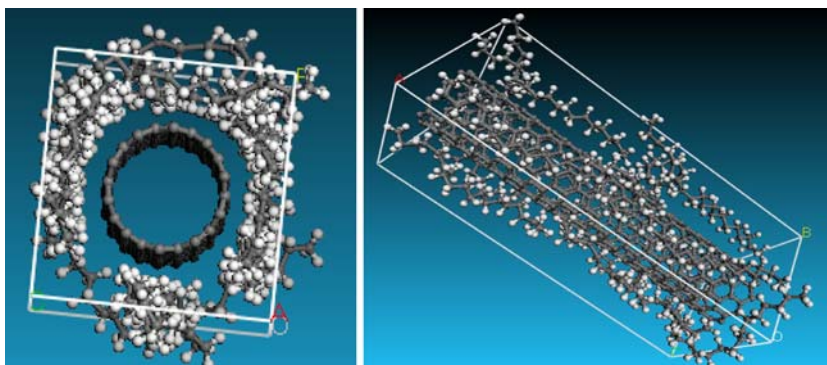




**Fig. 12** Molecular dynamics simulation cell for three 7,0 SWCNTs embedded in polyethylene matrix

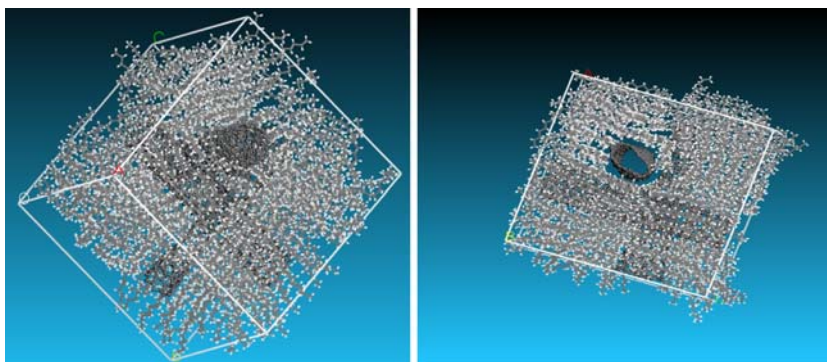


**Table 6** Engineering constants of simulated composite with three 7,0 SWCNTs randomly embedded in polyethylene matrix

$E$ (GPa)	$\nu_{12}$
24.62	0.36

In order to account for random distribution of CNTs in the polymeric matrix, molecular dynamics simulation was carried out for the three SWCNTs embedded in polyethylene matrix as shown in Fig. 12. The simulation cell for the composite consists of three single 7,0 SWCNTs embedded in the polyethylene matrix. The dimensions of the simulation cell were maintained as  $100 \text{ \AA} \times 100 \text{ \AA} \times 100 \text{ \AA}$ . Two step NPT molecular dynamics was applied. The temperature of the system was maintained at 298 K through out the simulation and a hydrostatic pressure of 1 atm pressure was applied to the system. The same volume fraction used in the case of single CNT embedded in polyethylene matrix was maintained with a total of 13,414 atoms used in the simulation. The engineering constants obtained as a result of this simulation are summarized in Table 6.

## Conclusions

Results obtained from various types of loadings applied to SWCNT show that SWCNTs are transversely isotropic. Elastic constants are the same for SWCNT under various loadings. Thus, SWCNT behaves as a linear elastic material. The simulation of various SWCNT clusters establishes the fact that clusters of nanotubes have lower transverse properties when compared to individual nanotubes. SWCNTs lose their circularity when a polymer chain is placed in their vicinity. This shows that their transverse properties are comparatively poor. The interface is an important constituent of CNT–polymer composites, which has been modeled in the present research with reasonable success.

**Acknowledgement** Authors wish to acknowledge partial support for this research by ONR Grant#N00014-06-1-0577, Office of Naval Research, Solid Mechanics Program (Dr. Yapa D.S. Rajapakse, Program Manager); and by the NASA EPSCoR Research Infrastructure Grant.

## References

- Deng CF, Wang DZ, Zhang XX, Li AB (2007) *Mater Sci Eng A* 444:138
- Yoon PJ, Fornes TD, Paul DR (2002) *Polymer* 43:6727
- Mishra S, Sonawane S, Chitodkar V (2005) *Polym Plast Technol Eng* 44:463–473
- Gilman JW, Jackson CL, Morgan AB, Harris R Jr (2000) *Chem Mater* 12:1866
- Strawhecker KE, Manias E (2000) *Chem Mater* 12:2943
- Krishnamoorti R, Vaia RA, Giannelis EP (1996) *Chem Mater* 8:1728
- Xu R, Manias E, Snyder AJ, Runt J (2001) *Macromolecules* 34:337
- Kojima Y, Usuki A, Kawasumi M, Okada A, Fukushima Y, Kurauchi T, Kamigaito O (1993) *J Mater Res* 8:1185
- Odegard GM, Gates TS, Nicholson LM, Wise C (2002) NASA ICASE report NASA/TM-2002-211454, March 2002
- Odegard GM, Gates TS, Nicholson LM, Wise C (2001) NASA ICASE report NASA/TM-2001-210863, May 2001
- Li C, Chou T (2003) *Int J Solids Struct* 40:2487
- Zhang P, Huang Y, Geubelle PH, Klein PA, Hwang K (2002) *Int J Solids Struct* 39:3893
- Zhang P, Huang Y, Gao H, Hwang K (2002) *Trans ASME* 69:454
- Arroyo M, Belytschko T (2004) *Phys Rev B* 69:115415.1
- Zhang P, Jiang H, Huang Y, Geubelle PH, Hwang KC (2004) *J Mech Phys Solids* 52:977
- Jiang H, Zhang P, Liu B, Huang Y, Geubelle PH, Gao H, Hwang KC (2003) *Comput Mater Sci* 28:429
- Jiang H, Feng XQ, Huang Y, Hwang KC, Wu PD (2004) *Comput Methods Appl Mech Eng* 193:3419
- Arroyo M, Belytschko T (2003) *Phys Rev Lett* 91(21):215505.1
- Tersoff J (1988) *Phys Rev B* 37:6991
- Brenner DW (1990) *Phys Rev B* 42:9458
- Yakobson BI, Cambell MP, Brabec CJ, Bernholc J (1997) *Comput Mater Sci* 8:341
- Belytschko T, Xiao SP, Schatz GC (2002) *Phys Rev B* 65(23):235430.1
- (2005) MS modeling 4.0 Online help manual, Accelrys Inc.
- www.wikipedia.org, the free web based encyclopedia, accessed on 05-01-2006
- Sun H (1998) *J Phys Chem B* 102:7338

26. Christensen R (1991) Mechanics of composite materials. Krieger Publishing Company, Malbar, Fl, p 74
27. Chou TW, Thostenson ET, Ren ZF (2001) *Composit Sci Technol* 61:1899
28. <http://www.pslc.ws/macrog/pe.htm>, Polymer science learning center, The University of Southern Mississippi
29. Gou J, Jiang S, Minaie B, Liang Z, Chuck Z, Wang B (2003) IMECE'03 – 41138, Proceedings of IMECE'03 international engineering congress and exposition. Washington, D.C., November 16–21, 2003, p 1
30. Liao K, Li S (2001) *Appl Phys Lett* 79(25):4225